Estuarine, Coastal and Shelf Science 87 (2010) 207–212

Contents lists available at ScienceDirect

Estuarine, Coastal and Shelf Science

journal homepage: www.elsevier.com/locate/ecss

Short communication

Combined effects of waves and plants on a mud deposition event at a mudflat-saltmarsh edge in the Bahía Blanca estuary

Paula D. Pratolongo [a,b,*], Gerardo M.E. Perillo [a,c], M. Cintia Piccolo [a,d]

[a] CONICET – Instituto Argentino de Oceanografía, CC 804, B8000FWB Bahía Blanca, Argentina
[b] Departamento de Biología, Bioquímica y Farmacia, Universidad Nacional del Sur, San Juan 670, B8000DIC Bahía Blanca, Argentina
[c] Departamento de Geología, Universidad Nacional del Sur, San Juan 670, B8000DIC Bahía Blanca, Argentina
[d] Departamento de Geografía y Turismo, Universidad Nacional del Sur, 12 de Octubre y San Juan, 8000 Bahía Blanca, Argentina

ARTICLE INFO

Article history:
Received 31 August 2009
Accepted 22 September 2009
Available online 12 October 2009

Keywords:
mudflats
saltmarsh
sediment deposition
Bahía Blanca
Argentina

ABSTRACT

This study was carried out at the Bahía Blanca Estuary, Argentina, at the seaward edge of a saltmarsh. The saltmarsh-mudflat boundary in the study area shows sediment deposits at a higher elevation immediately seaward of the saltmarsh edge. We compared field determinations of water velocity, bed shear stress, wind wave conditions and variations of the bed elevation in the mudflat and within the *Spartina alterniflora* canopy at the seaward edge of a saltmarsh, and we evaluated the relative role of vegetation in the observed morphology. A mud deposition event that raised bed elevation in more than 5 cm occurred during the study period, with TSS concentrations $> 500\ mg\ l^{-1}$, but simultaneous measurements performed on the bed levels confirmed that the sediments deposited did not originate from local resuspension within the edge of the canopy. In similar tidal cycles in terms of local wave activity and bed shear stresses at the sampling site, deposition occurred only with winds aligned with the azimuth of the Canal Principal, reaching a maximum fetch of more than 20 km in front of the sampling site.

1. Introduction

Saltmarshes and mudflats often occupy extensive intertidal areas along sheltered coasts. As transition zones between continents and oceans, they play a major role in the exchange of organic matter, and may act as both sources and sinks for fine sediments (Gordon et al., 1985). Given their commonly high net primary production, biomass exported from salt marshes and mudflats is often considered the basis for food webs in coastal waters (Chalmers et al., 1985). Because of the important ecosystem services provided by mudflats and saltmarshes, there is a growing concern over their vulnerability, especially under enhanced sea-level rise scenarios or increased storminess. However, it is still not clear in which way tidal currents, waves, sediment erosion or deposition, and saltmarsh plants interact, and how these interactions result in morphological changes (Widdows et al., 2008). Such knowledge is a fundamental prerequisite for a sustained management of these environments in the future.

Several laboratory and field studies have shown that saltmarsh canopies radically modify the flow structure. It has been found that saltmarsh plants significantly attenuate tidal currents and waves (Leonard and Luther, 1995; Möller, 2006) and, in some cases, saltmarshes provide a natural coastal defense by dissipating energy from high tides and storms (Perillo, 2009; Wolanski et al., 2009). Leonard and Croft (2006), for instance, demonstrated the effects of *Spartina alterniflora* in attenuating tidal flows and small waves close to the edge of a saltmarsh. Similar results were found by Moeller et al. (1999) who measured large reductions in wave heights over a more diverse salt marsh canopy. However, the conditions for sedimentation are not clear. Although it is generally observed that sedimentation rate increases with increasing vegetation density (French et al., 1995), sediment erosion has also been observed along some saltmarsh edges (Pethick et al., 1990).

In addition, an increased wave activity has been related to both an enhanced sedimentation and bed erosion on the marsh platform (Widdows et al., 2008). In the Bay of Fundy, van Proosdij et al. (2006) proposed that wave activity increases suspended sediment concentrations and transport further up onto the mid to upper marsh. In contrast, Pethick (1992) found that storms in Essex, UK may result in erosion of the outer and lower parts of the saltmarshes when waves are effectively propagated into the estuary, or when locally produced waves reach sufficient height.

* Corresponding author. CONICET – Instituto Argentino de Oceanografía, CC 804, B8000FWB Bahía Blanca, Argentina.
E-mail address: ppratolongo@gmail.com (P.D. Pratolongo).

0272-7714/$ – see front matter © 2009 Elsevier Ltd. All rights reserved.
doi:10.1016/j.ecss.2009.09.024

In the Bahía Blanca Estuary, Argentina, *Spartina alterniflora* marshes occur as discontinuous patches near the neap high-tide level (Pratolongo et al., 2009). The sediment surface reveals a repetitive and conspicuous morphology produced by elevated patches of bare mud within the vegetation, as well as sediment deposits at higher elevations immediately seaward of the saltmarsh edge. In this paper we compare field determinations of near bed currents, wind wave conditions and variations in bed elevation in the mudflat and within the *S. alterniflora* canopy at the seaward edge of a saltmarsh. The purpose of these observations was to establish the relative role of vegetation in the resulting morphology. In this context, we tested the hypothesis that in the study site, sediment retention does not primarily occur within the marsh, but rather on the adjacent mudflat.

2. Study area

The Bahía Blanca estuary (Fig. 1) is a mesotidal system formed by a series of major channels running from the northwest to the south-east. Canal Principal is the main channel in the estuary, having a total length of 60 km and a width ranging from 200 m at the head to more than 3 km at the mouth (Perillo and Piccolo, 1999). The present study was carried out near Villa del Mar, a coastal town located in the middle-outer reach of the Canal Principal where the mean tidal range is 3.5 m. The whole region is affected by strong and persistent north-westerly and northerly winds with mean velocities around 24 km h^{-1} and gusts over 100 km h^{-1} (Piccolo and Perillo, 1999). In front of the study site, effective fetches for these dominant winds exceed 20 km.

Off Villa del Mar, the intertidal mudflat covers about 6 km^2, and extends for more than 1 km across the tidal gradient. Bed sediments are a mixture of mud and sand (87% and 13%, respectively) having modal diameters of 12 and 130 μm. Close to the mean high-tide level, *Spartina alterniflora* marshes form a narrow, 150 m wide strip of vegetation. The marsh topography is characterized by a very gently sloping ramp on the seaward side and a steeper slope at the landward edge where it is commonly replaced by bare saltflats or *Sarcocornia perennis* marshes (Pratolongo et al., 2009). A peculiar feature of this area is the total absence of tidal creeks and channels, with the exchange of tidal water and suspended sediments taking place across the entire saltmarsh front.

The bed morphology at the saltmarsh/mudflat boundary often shows a higher elevation on the bare mudflat immediately seaward of the saltmarsh edge. These deposits commonly occur in large patches separated by a step-like depression or moat from the lower limit of the vegetation. Field observations suggest that deposition of a large volume of sediments in this zone occurs in discrete events such as strong prolonged winds or storms.

3. Methods

3.1. Field measurements

The general topography of the marsh/tidal flat complex was originally surveyed by means of a theodolite and later controlled and corrected with a DGPS-RTK. Hydrodynamic measurements near the bed were carried out in February 2007, during a spring-neap tidal cycle, by the simultaneous deployment of two Sontek (10 MHz) acoustic Doppler velocimeters (ADVs) at the saltmarsh edge, one sensor mounted over the bare mudflat, and the other one 1 m landward within the fringe of the saltmarsh canopy. Both devices were fixed on a single, rigid stainless steel tetrapod, designed and positioned to minimize frame-induced interferences.

The ADVs included a compass and a pressure sensor, and were programmed to register the three directional components of the current velocity as well as water level variations at 10 Hz, in 12 m bursts, every 20 min. Based on previous unpublished data, we decided to sample currents and waves at 10 Hz because the tidal currents in this area are relatively small and do not generate turbulent conditions. Furthermore, surface waves and the energy-containing scales of the turbulence occupy much lower frequencies.

At the beginning of the measurements, the sampling volumes for the velocity components were located 10 cm above the bed, and the distance from the sampling volume to the ground was registered at the beginning of every burst. Velocities were recorded in the East (u)/North (v)/Up (w) coordinates, and automatically compensated for misalignment of the instrument using the ADV internal compass.

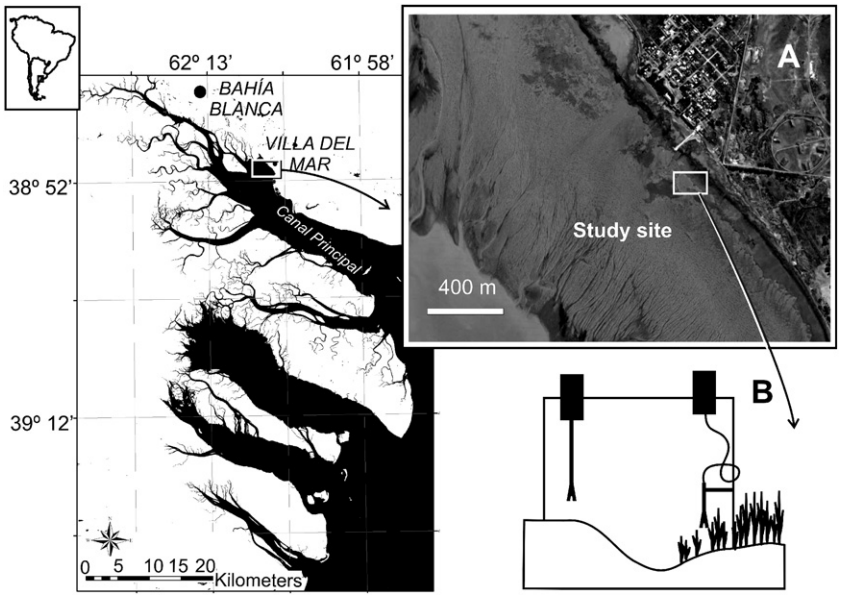

Fig. 1. The Bahía Blanca estuary in south-eastern South America. The aerial photograph (A) shows a detail of the study area at Villa del Mar, an extensive mudflat located in the middle-outer reach of the Canal Principal. Two ADVs were deployed at a saltmarsh-mudflat boundary (B) to perform simultaneous near-bed measurements over the bare mudflat and twithin the edge of the canopy.

In addition, surface sediment samples were collected at the beginning of the measurements, and meteorological data were obtained throughout the sampling period from a meteorological station located 100 m from the field site.

3.2. Total suspended solids (TSS) estimations

ADVs use acoustic backscatter to estimate flow velocities. Since the intensity of the returned sound for each acoustic beam is also recorded by the sensor, and the intensity is proportional to the concentration and size of sound scatterers in the sample volume, it is also possible to estimate TSS concentrations after appropriate calibration (e.g. Fugate and Friedrichs, 2002; Voulgaris and Meyers, 2004). However, calibrating the backscattered acoustic intensity with TSS concentrations is complex and depends not only on the TSS but also grain-size distribution, composition, and the presence of aggregates in the volume sampled. The backscatter intensity is also affected by turbulence and is thus a combination of signals produced by both suspended solids and noise. In spite of the present uncertainties, several authors have achieved reasonable success in applying acoustic backscatter as a proxy for TSS utilizing empirical calibrations (Thevenot and Kraus, 1993; Kawanisi and Yokosi, 1997). In this study, we used an empirical calibration as proposed by Voulgaris and Meyers (2004) to convert the backscatter signal to TSS concentration.

The calibration experiment was carried out in the laboratory using surface sediments collected at the sampling site. The ADVs were immersed in a water-filled tank; sediment was then added in discrete quantities and homogenized to obtain a stepwise increase in the TSS concentration. The backscattered intensities were recorded in 60 s bursts. At the end of every burst, a water sample was collected and filtered, and the dry weight of TSS determined. Finally, the calibration curve was obtained by log-log linear correlation between the sampled TSS concentrations and the burst-averaged values of the backscattered acoustic intensity.

3.3. Data analysis

Pressure time series were filtered to remove any low-frequency tidal components. According to the linear theory (Tucker and Pitt, 2001), we applied a frequency-dependent correction in the range 0.05–0.33 Hz to account for signal attenuation with depth. For each burst, the zero-crossing period (Tz) and the significant wave height (Hs) were derived from the filtered data. The total wave energy (E_{tot}) was calculated from the spectral variance.

To estimate the wave induced bottom shear stress, a spectral analysis of the instantaneous velocities was carried out to separate the wave-induced and turbulence-induced variances on each component (Soulsby and Humphery, 1990). During wave events, the energy spectrum presents the Kolmogorov −5/3 roll-off in the inertial subrange and a superimposed energy peak in the wave frequency range (typically between 1 and 0.1 Hz for wind waves). Following Soulsby and Humphery (1990), the energy spectrum was split at the base of the wave peak to obtain the wave variances (u_w',v_w',w_w') of each fluctuating velocity component (u′,v′,w′).

The significant wave orbital velocity (U_w) was calculated from the wave variances according to Myrhaug et al. (1998):

$$U_w = 2\sqrt{\overline{u_w'^2} + \overline{v_w'^2}}.$$

The wave shear stress (τ_w) was estimated as:

$$\tau_w = 0.5\,\rho\, f_w\, U_w^2,$$

with f_w as the wave friction factor estimated as suggested by Soulsby (1997) for turbulent flow:

$$f_w = 1.39(A/z_0)^{-0,52},$$

where A is the semi-orbital excursion calculated from

$$A = \frac{U_w\ T_z}{2\pi}$$

Bed roughness length (z_0) varies with different sediment grain size distribution, the presence of bedforms, and changes in suspended sediment concentration (Voulgaris and Meyers, 2004). Although its variations should be determined throughout the sampling period, in the presence of waves z_0 is greatly affected by the increase in eddy viscosity within the wave boundary layer (Grant and Madsen, 1979) and no longer corresponds to the physical bed roughness that has to be used to calculate bottom shear stress. In some cases (e.g. Verney et al., 2007), the bed roughness length can be estimated from the drag coefficient, outside wave events, and assuming a logarithmic velocity profile (Soulsby and Humphery, 1990). In our study, wave activity was continuously present during the sampling period, so we could not estimate the actual values for z_0. Instead, we assumed the linear relationship $z_0 = 3\ D_{50}$, as suggested by Voulgaris and Meyers (2004) for mud-sand mixtures in mudflats with no topographic effect.

4. Results

The topographic profile across the intertidal fringe reveals a pronounced break in the slope at the lower limit of the vegetation. Towards the seaward edge, *Spartina alterniflora* becomes less dense and shorter, and the boundary between the marsh and the mudflat is well defined by a small depression and the presence of an elevated levee on the mudflat side. A plane and bare saltflat develops landward of the *S. alterniflora* marsh, close to the level of the spring high tides. Further inland, a narrow strip of high marsh is covered by plants less tolerant to tidal flooding (*Spartina densiflora, Sarcocornia perennis* and *Distichlis spicata*).

The experimental derived relationship between the ADV backscattered amplitude and TSS concentration showed that the correlation between log [TSS] and log [backscattered amplitude] was statistically significant ($\rho = 0.92$, $p < 0.01$). The measured concentrations ranged from 40 to 3976 mg l^{-1} and the obtained calibration curve was

$$\log\,[\mathrm{TSS}] = 8.1635 \times \log[\mathrm{backscatter}] - 15.225$$

Wave activity was present in every burst recorded during the sampling period, as denoted by conspicuous peaks in the energy spectrum at frequencies between 1 and 0.1 Hz. During the sampled spring-neap tidal cycle, τ_W was commonly an order of magnitude higher than τ_{TKE} normally obtained in similar conditions, with maximum values above 4 N m^{-2}. The largest values of τ_W were clearly associated with high-energy wave events, the waves being typically in the range from 10 to 20 cm in height and larger than 1.5 s in period.

Higher TSS concentrations were related to τ_W values above 1 N m^{-2}. This may be due to local resuspension of sediments once the critical erosion threshold was exceeded. However, the distance to the bed surface recorded at the beginning of every burst did not show any significant variation during these periods, suggesting that the higher turbidity was not associated with local erosion.

The data illustrated in Fig. 2 correspond to the measurements obtained from 24 to 26 February 2007 and comprise a total of five tidal cycles showing interesting combinations of wave activity and changes in bed level. The absence of data at levels below 80 cm is

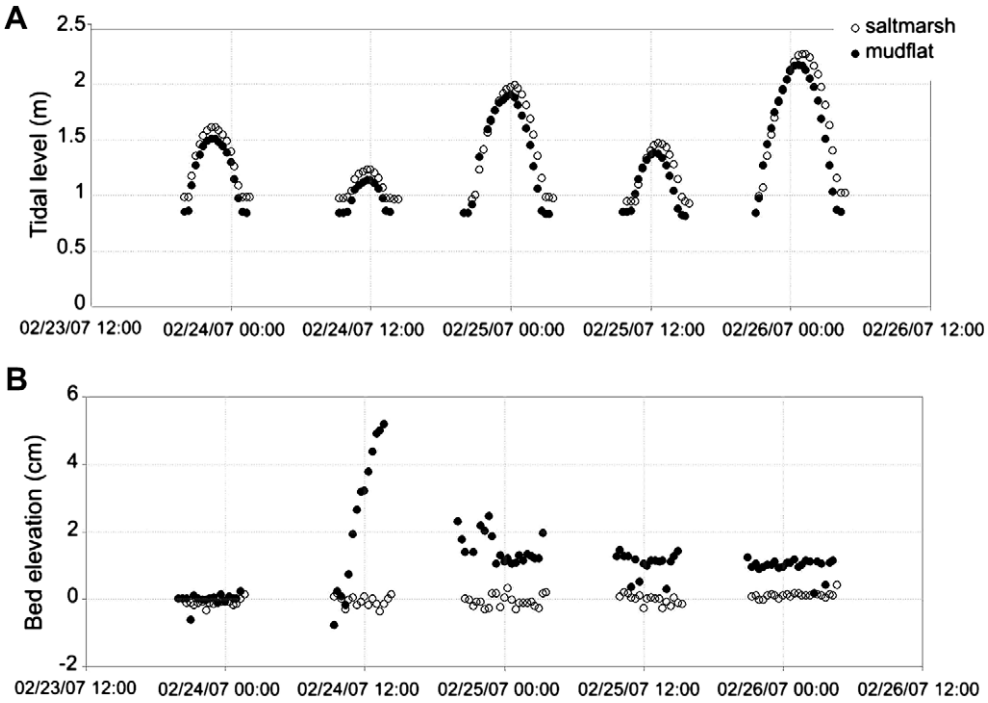

Fig. 2. Tidal levels at the sampling sites (A). Each value corresponds to water depths averaged over a burst cycle. Levels are in meters above the surface. Bed elevations at both sampling sites (B). Values refer to the levels at the beginning of each measurement period. Positive values indicate elevations higher that the first level recorded (deposition).

due to the fact that the position of the pressure sensor was 70 cm above the sampling volume.

During the first inundation cycle, on the night of February 24, bed levels at the marsh edge and the mudflat showed little change. However, remarkable differences appeared at the beginning of the following tidal inundation when the bed level of the mudflat progressively increased by up to 5 cm above the original level, whereas no significant changes, i.e. neither erosion nor deposition, were registered on the marsh surface. Immediately after this deposition event, a period of aerial exposure occurred from 13:52 in the afternoon to 20:00 in the evening when bed elevations could not be registered. At the beginning of the next inundation, the bed level of the mudflat was 2.89 cm below the level registered previously, probably due to compaction and dehydration (air temperatures during the exposure ranged from 18.1 to 22.3 °C). Bed elevation continued to drop through the tidal cycle until a new level was established around 1 cm above the original elevation, which was maintained with small oscillations up to the end of the study.

Two different high-energy tidal cycles can be identified during the sampling period showed in Fig. 2, these correlating with sustained wind speeds above 20 km h^{-1} (Table 1). Although wave conditions, τ_W and TSS were similar for both periods, a significant depositional event only occurred on February 24. A distinctive feature of this event were sustained winds blowing from the northwest, along the azimuth of Canal Principal, at a mean speed of 33 km h^{-1} and gusts of over 50 km h^{-1}.

5. Discussion

The field measurements reveal that wind-waves are a major hydrodynamic forcing factor above the mudflats in the study area. During the survey, short waves (periods from 1 to 3 s) were observed continuously during the tidal cycle. Although significant wave heights never exceeded 20 cm, these waves produced bottom shear stresses as high as 4 N m^{-2} in this shallow water environment. This is one order of magnitude higher than the current-induced bottom shear stresses estimated during this and previous (unpublished) studies. These results agree with previous observations by Perillo and Sequeira (1989) who found that typical wind waves of about 10 cm in height, maximum wavelengths of 1–3 m, and periods of 1–3 s characterize the hydrodynamics of the intertidal flats during high tide. Moreover, wind forcing is known to have large effects on tidal flow patterns, significant tidal anomalies being commonly related to regional winds (Piccolo et al., 2008).

A remarkable finding throughout the survey was that marsh plants neither attenuated the near-bed currents nor dampened the waves similar to what was found by Moeller et al. (1999), who had their sensors at about the same distance from the edge of the marsh. On the contrary, at times both the τ_W and the wave energy were even higher over the marsh as compared to the bare mudflat. *Spartina spp.* marshes are often described as ecosystem engineers because of their capacity to increase sediment accretion and thereby change bed elevation (e.g. Allen, 1990; Christiansen et al., 2000). In the present case, a significant depositional event comprising a 5 cm thick layer of mud was recorded in the course of a single tidal cycle along the saltmarsh front just seaward of the lower limit of the vegetation. However, contrary to common perception, deposition did not occur within the marsh canopy. In fact, 3 years of unpublished Surface Elevation Table (SET after Cahoon et al., 2002) data from the studied marsh (the SET is located less than 100 m from the ADVs, at a slightly higher elevation) show little variation over time, with no evidence of net sediment accumulation on the surface, but mild erosion.

The morphology in the wider study area reveals that this depositional pattern is not an isolated local feature but rather a common process on the entire mudflat along the middle-outer reach of the Canal Principal. Most of the sediments in the estuary are being reworked from the original Colorado River delta since there are no sediment inputs from either major rivers or the inner shelf. Therefore, tidal flats and marshes in the head of the estuary

Table 1
Wave characteristics estimated for every burst within a tidal flood, at each sampling site. Values correspond to the median (peak) over each tidal flood. Parameters are: (Tz) significant zero-crossing period, (Hs) significant wave height, (E_{tot}) total wave energy, estimated from the spectral variance, (τ_W) bed shear stress caused by waves, and (TSS) total suspended solids concentrations estimated from the backscatter amplitude.

	Tidal flood 1		Tidal flood 2 (deposition event)		Tidal flood 3		Tidal flood 4		Tidal flood 5	
Start time	2/23/2007 20:00		2/24/2007 9:20		2/24/2007 20:00		2/25/2007 9:40		2/25/2007 21:00	
End time	2/24/2007 1:20		2/24/2007 13:40		2/25/2007 3:20		2/25/2007 15:00		2/26/2007 4:20	
Wind speed ($km\,h^{-1}$)	13		39		21		10		32	
Wind direction	N		NW		E		NE		SE	
	Marsh	Mudflat	Marsh	Mudflat	Marsh	Mudflat	Marsh	Mudflat	Marsh	Mudflat
Tz (s)	1.01(1.5)	0.92(1.8)	1.53(2.0)	1.66(2.0)	0.79(1.4)	0.68(1.3)	0.71(1.6)	0.68(1.4)	2.26(3.0)	2.20(3.0)
Hs (cm)	3.25(5.60)	3.20(5.07)	9.84(20.65)	9.58(18.60)	2.74(6.21)	2.90(6.67)	2.74(3.34)	2.78(3.32)	8.88(16.89)	8.08(17.00)
E_{tot} ($J\,m^{-2}$)	0.11(0.37)	0.13(0.24)	0.59(11.05)	1.20(8.72)	0.09(0.36)	0.09(0.36)	0.06(0.82)	0.06(0.59)	3.68(13.54)	3.33(12.20)
$\tau\, w$($N\,m^{-2}$)	0.11(0.62)	0.08(0.58)	0.87(3.63)	0.88(3.59)	0.06(0.80)	0.06(1.24)	0.05(0.23)	0.05(0.21)	0.40(4.36)	0.35(3.86)
TSS ($mg\,l^{-1}$)	61(165)	40(99)	415(694)	400(529)	60(305)	36(234)	47(91)	31(50)	288(860)	193(617)

are the main suppliers of sediments by direct erosion due to wave action, and Canal Principal is the main channel driving these sediments out of the estuary.

High TSS concentrations estimated from ADV backscatter intensity were closely related to high-energy wave events, suggesting that wave action is responsible for erosion and/or resuspension processes. However, the boundary condition (distance to the bottom) measured at the beginning of every burst did not reflect a significant lowering of the bed elevation during such events. Verney et al. (2007) found a similar discrepancy when comparing TSS estimations from backscatter intensity with measurements of bed levels using an acoustic altimeter. An explanation suggested in that case was that erosion only involved a thin layer of mud and that the lowering of the bed surface was smaller than the vertical resolution of the instrument. While this may have been the case in the last tidal cycle shown in Fig. 2, a major depositional event of more than 5 cm occurred during the second flood tide, this being associated with some of the highest TSS concentrations ($>500\,mg\,l^{-1}$) recorded throughout the survey.

As we did not have any instruments farther offshore on the tidal flat, we assume that during the depositional event described here, the increase in TSS recorded by the ADV was more likely the result of bed erosion off the study site, and the resuspended sediments being advected shoreward where it was recorded by the ADV. Indeed, a distinctive feature of that tidal cycle was the occurrence of sustained winds blowing from the northwest, the main wind direction of the region (Piccolo, 2008). These strong winds are aligned with the azimuth of the Canal Principal, reaching a maximum fetch of more than 20 km in front of the sampling site. As a result of the long fetch, longer waves are generated which appear to cause bed liquefaction (Mehta, 1996) in the channel. The fluid mud mobilized in this way would then be transported onshore by the tidal currents until the sediment reaches the edge of the canopy where it would be deposited.

A similar morphology in the form of a depression and shoulder at the front edge of a *Spartina anglica* saltmarsh in the Tavy estuary, southwest England has been described by Widdows et al. (2008). In their study, they also found a consistent pattern of higher sedimentation on bare mudflats. Based on flume experiments on the critical bottom shear stress for erosion and field measurements on τ_{TKE} and turbidity, these authors found that the enhanced turbulent kinetic energy between *S. anglica* stems precluded particle settling within the canopy. In addition, they performed monthly measurements on the depression-shoulder profile, finding that the greatest changes in sediment levels occurred under conditions of strong wind wave activity. However, they suggest that the enhanced turbulence at the edge of the marsh is responsible for the lowering of the bed level and, as the maximum bed shear stress occurs at the end of the ebb tide, part of the resuspended sediments would be deposited in front of the marsh, raising the shoulder.

There are several remarkable similarities between the mudflat of the Tavy estuary and the study site at Villa del Mar. In both cases, extensive soft mudflats extend over large distances across the elevation gradient, and *Spartina spp*. marshes do not develop tidal creeks or channel networks. In addition, wind waves are described as the dominant hydrodynamic force with the larger fetches for the dominant wind directions. In our case, however, simultaneous measurements of bed levels during a depositional event effectively confirmed that the deposited sediments could not have originated from local resuspension within the edge of the canopy. Moreover, similar depositional events always occurred when the wind direction was such that it generated larger waves in the main channel, whereas no depositional effects were observed in association with winds from other directions with shorter fetch.

Finally, due to the almost continuous presence of waves, real values of the bed roughness lengths to be used in τ_W calculations could not be calculated. The use of a single constant value through successive tidal cycles may produce large errors in the estimations (as shown by Verney et al., 2007), especially at higher current velocities. Given the dynamic nature of the system characterized by successive periods of sedimentation and thus changes in sediment properties, more accurate field determinations of the bed roughness should be attempted in future surveys.

Acknowledgments

We wish to especially thank Eng. Alejandro Vitale for field support as well as for the valuable assistance with data processing. We also thank Dr. Walter Melo for providing cartographic data. Comments by two anonymous reviewers were very helpful to improve the manuscript. This work was partly supported by grants from CONICET (PIP 5017), ANPCyT (PICTs 1726 and 25705), and Universidad Nacional del Sur (PGI 24/H082). SCOR/LOICZ/IAPSO WG 122 on Mechanisms of Sediment Retention in Estuaries was sponsored by SCOR, LOICZ, U.S. National Science Foundation

References

Allen, J.R.L., 1990. Salt marsh growth and stratification: a numerical model with special reference to the Severn estuary, southwest Britain. Marine Geology 95, 77–96.

Cahoon, D.R., Lynch, J.C., Hensel, P., Boumans, R., Perez, B.C., Segura, B., Day Jr., J.W., 2002. A device for high precision measurement of wetland sediment elevation: I. Recent improvements to the sedimentation-erosion table. Journal of Sedimentary Research 72, 730–733.

Chalmers, G.C., Wiegert, R.G., Wolff, P.L., 1985. Carbon balance in a salt marsh: interactions of diffusive export, tidal deposition and rainfall-caused erosion. Estuarine Coastal and Shelf Science 21, 757–771.

Christiansen, T., Wiberg, P.L., Milligan, T.G., 2000. Flow and sediment transport on a tidal salt marsh surface. Estuarine Coastal and Shelf Science 50, 315–331.

French, J.R., Spencer, T., Murray, A.L., Arnold, N.S., 1995. Geostatistical analysis of sediment deposition in two small tidal wetlands, Norfolk, U.K. Journal of Coastal Research 11 (2), 308–321.

Fugate, D., Friedrichs, C.T., 2002. Determining concentration and fall velocity of estuarine particle populations using ADV, OBS, and LISST. Continental Shelf Research 22, 1867–1886.

Gordon, D.C., Cranford, P.J., Desplanque, C., 1985. Observations on the ecological importance of salt marshes in the Cumberland Basin, a macrotidal estuary in the Bay of Fundy. Estuarine Coastal and Shelf Science 20, 205–227.

Grant, J., Madsen, O.S., 1979. Combined wave and current interaction with a rough bottom. Journal of Geophysical Research 84 (C4), 1797–1808.

Kawanisi, K., Yokosi, S., 1997. Characteristics of suspended sediment and turbulence in a tidal boundary layer. Continental Shelf Research 17 (8), 859–875.

Leonard, L.A., Luther, M.E., 1995. Flow hydrodynamics in tidal marsh canopies. Limnology and Oceanography 40 (8), 1474–1484.

Leonard, L.A., Croft, A.L., 2006. The effect of standing biomass on flow velocity and turbulence in *Spartina alterniflora* canopies. Estuarine Coastal and Shelf Science 69, 325–336.

Mehta, A.J., 1996. Interaction between fluid mud and water waves. In: Singh, V.P., Hager, W.H. (Eds.), Environmental Hydraulics. Kluwer, Dordretcht, pp. 153–187.

Moeller, I., Spencer, T., French, J.R., Leggett, D.J., Dixon, M., 1999. Wave transformation over salt marshes: a field and numerical modeling study from North Norfolk, England. Estuarine Coastal and Shelf Science 49, 411–426.

Möller, I., 2006. Quantifying saltmarsh vegetation and its effect on wave height dissipation: results from a UK East coast saltmarsh. Estuarine Coastal and Shelf Science 69 (3–4), 337–351.

Myrhaug, D., Slaattelid, O.H., Lambrakos, K.F., 1998. Seabed shear stresses under random waves: prediction vs estimates from field measurements. Ocean Engineering 25 (10), 907–916.

Perillo, G.M.E., 2009. Tidal courses: classification, origin and functionality. In: Perillo, G.M.E., Wolanski, E., Cahoon, D.R., Brinson, M.M. (Eds.), Coastal Wetlands: An Integrated Ecosystem Approach. Elsevier, Amsterdam, pp. 185–210.

Perillo, G.M.E., Piccolo, M.C., 1999. Geomorphologic and physical characteristics of the Bahía Blanca Estuary, Argentina. In: Perillo, G.M.E., Piccolo, M.C., Pino Quivira, M. (Eds.), Estuaries of South America: Their Geomorphology and Dynamics. Springer-Verlag, Berlin, pp. 195–216.

Perillo, G.M.E., Sequeira, M.E., 1989. Geomorphologic and sediment transport characteristics of the middle reach of the Bahía Blanca estuary, Argentina. Journal of Geophysical Research-Oceans 94, 14351–14362.

Pethick, J.S., 1992. Saltmarsh geomorphology. In: Allen, J.R.L., Pye, K. (Eds.), Saltmarshes: Morphodynamics, Conservation and Engineering Significance. Cambridge University Press, Cambridge, pp. 41–62.

Pethick, J.S., Legget, D., Husain, L., 1990. Boundary layers under saltmarsh vegetation developed in tidal currents. In: Thorne, J.B. (Ed.), Vegetation and Erosion. Wiley, Chichester, UK, pp. 113–123.

Piccolo, M.C., Perillo, G.M.E., 1999. Estuaries of Argentina: a review. In: Perillo, G.M.E., Piccolo, M.C., Pino Quivira, M. (Eds.), Estuaries of South America: Their Geomorphology and Dynamics. Springer-Verlag, Berlin, pp. 101–132.

Piccolo, M.C., 2008. Climatological features of the Bahía Blanca estuary. In: Neves, R., Baretta, J.W., Mateus, M. (Eds.), Perspectives on Integrated Coastal Zone Management in South America. IST Press, Lisboa, pp. 231–240.

Piccolo, M.C., Perillo, G.M.E., Melo, W.D., 2008. The Bahía Blanca estuary: an integrated overview of its geomorphology and dynamics. In: Neves, R., Baretta, J.W., Mateus, M. (Eds.), Perspectives on Integrated Coastal Zone Management in South America. IST Press, Lisbon, pp. 219–230.

Pratolongo, P., Kirby, J., Plater, A., Brinson, M., 2009. Temperate coastal wetlands: morphology, sediment processes, and plant communities. In: Perillo, G.M.E., Wolanski, E., Cahoon, D.R., Brinson, M.M. (Eds.), Coastal Wetlands: An Integrated Ecosystem Approach. Elsevier, Amsterdam, pp. 185–210.

van Proosdij, D., Ollerhead, J., Davidson-Arnott, R.G.D., 2006. Seasonal and annual variations in the volumetric sediment balance of a macro-tidal salt marsh. Marine Geology 225 (1–4), 103–127.

Soulsby, R.L., Humphery, J.D., 1990. Field observations of wave–current interaction at the sea bed. In: Torum, A., Gudmestad, O.T. (Eds.), Water Wave Kinematics. Kluwer Academic Publishers, Dordrecht, pp. 413–428.

Soulsby, R.L., 1997. Dynamics of Marine Sands. A Manual for Practical Applications. Thomas Telford, London, p. 249.

Thevenot, M.M., Kraus, N.C., 1993. Comparison of acoustical and optical measurements of suspended material in the Chesapeake Estuary. Journal of Marine Environmental Engineering 1, 65–79.

Tucker, M.J., Pitt, E.G., 2001. Waves in ocean engineering. In: Bhattacharyya, R., McCormick, M.E. (Eds.), Elsevier Ocean Engineering Book Series 5. Elsevier, Amsterdam, p. 521.

Verney, R., Deloffre, J., Brun-Cottan, J.C., Lafite, R., 2007. The effect of wave-induced turbulence on intertidal mudflats: impact of boat traffic and wind. Continental Shelf Research 27, 594–612.

Voulgaris, G., Meyers, S.T., 2004. Temporal variability of hydrodynamics, sediment concentration and sediment settling velocity in a tidal creek. Continental Shelf Research 24 (15), 1659–1683.

Widdows, J., Pope, N., Brinsley, M., 2008. Effect of Spartina Anglica stems on nearbed hydrodynamics, sediment erodability and morphological changes on an intertidal mudflat. Marine Ecology Progress Series 362, 45–57.

Wolanski, E., Brinson, M.M., Cahoon, D.R., Perillo, G.M.E., 2009. Coastal wetlands: a synthesis. In: Perillo, G.M.E., Wolanski, E., Cahoon, D.R., Brinson, M.M. (Eds.), Coastal Wetlands: An Integrated Ecosystem Approach. Elsevier, Amsterdam, pp. 1–61.